RIS-Aided Highly Directional Millimeter-Wave Communications: Power and Beamwidth Control

Yuan Cao, Wei Peng, *Senior Member, IEEE*, Chau Yuen, *Fellow, IEEE*

***Abstract*—Reconfigurable Intelligent Surface (RIS) is considered as a technology capable of artificially modify the wireless channel, then the communication performance might be improved in terms of the coverage and the signal strength. Most studies focus on the omni-directional communication systems operating in the sub-6 GHz band and assume that the RIS can be fully illuminated. However, in future highly directional millimeter-wave communication systems, the beamwidth emitted by the base station (BS) is very narrow, and only a part of the RIS elements, instead of full of them, will be illuminated. As a result, the signal power and the RIS reflected beamwidth will decrease. In addition, random failures of RIS units may introduce phase shift errors, which will degrade the received signal power. To address these problems, in this paper, the RIS illuminated area will be optimized through rotation. Specifically, the illuminated area as a function of the rotation angle is explicitly analyzed, and closed-form expressions for the optimal rotation angle and the critical rotation angle are derived. The effectiveness of the proposed scheme is verified by simulation results, which demonstrate that, the received signal power can be improved. The RIS reflected beamwidth can be increased to four times compared to its original size in our simulation setup, while maintaining the same received power, thus allowing an enlarged receiving area.**

***Index Terms*—Millimeter-wave communication, high directionality, reconfigurable intelligent surface, beamwidth, rotation**

I. Introduction

WITH the acceleration of digital transformation, the growing number of various services and high-speed terminal devices has almost exhausted the resources of the current Sub-6 GHz frequency band. High-frequency bands have abundant bandwidth resources that can support new mobile application scenarios [1]. However, the millimeter wave band suffers from severe path loss, and obstacles will cause significant signal attenuation. An effective solution is the use of reconfigurable intelligent surface (RIS), which is usually a two-dimensional plane composed of a large number of passive units that can manipulate electromagnetic waves. Each RIS unit can reflect electromagnetic waves, constructively focusing them on the receiving end to enhance the system performance.

Deploying RIS near the base station (BS) or user equipment (UE) can achieve a high signal-to-noise ratio, as indicated in [2]. Furthermore, it reveals that the optimal position of RIS for maximizing the received signal power is not always near the BS or the UE, but rather depends on the geometric structure composed of the BS, UE and RIS [3]. The optimal RIS placement in highly-directional millimeter-wave links to maximize signal-to-noise ratio is studied in [4].

Additionally, the orientation of RIS also affects the system performance significantly. It is shown that the effective area of the RIS is determined by its orientation [5]. A RIS placement problem is formulated, and a coverage maximization algorithm is proposed by jointly optimizing the RIS orientation and the distance between the BS and the RIS in [6]. In our previous work, the position and rotation angle of RIS are jointly optimized to enhance the system performance [7]. Closed form expressions of the optimal rotation angles are further derived for two-dimensional rotation scheme in multi-hop RISs assisted wireless communication systems [8]. A rotatable block-controlled RIS achieves the same spectral efficiency as unit-controlled RIS but with fewer phase shifters [9]. A dynamic rotation method is proposed to maximize the cascaded channel gain between the transmitter and the receiver [10]. An off-center optimization method is proposed to compensate for the decrease in received power caused by rotation errors [11].

The studies mentioned above all applied to the omni-directional communication systems and assumed that the RIS can be fully illuminated. However, in future communication systems, high-frequency band such as the millimeter wave and Tera Hz will become a powerful candidate. In addition, a high-directional beam pattern will be used in BS. As a result, only a portion of the RIS units will be illuminated, which depends on the transmit beamwidth and the distance between the BS and the RIS [12]. In this paper, the RIS-aided millimeter-wave communication systems with high directionality is considered. To our best acknowledge, this is the first work to improve the system performance under the partially illuminated condition. The main contributions are as follows.

- The received signal power is formulated as a function of the illuminated RIS area, and the optimal solution is then obtained by RIS rotation. Specifically, considering the far-field beamforming, the impact of the RIS down tilt angle on the illuminated area and the received signal

Manuscript received XX XX, 2025; revised XX XX, 2025. This work was supported in part by the National Natural Foundation of China under Grant 2171192, the International Cooperation Project of Shenzhen Science and Technology Innovation Commission under grant GJHZ20220913143401002, and the Fundamental Research Funds for the Central Universities, HUST: 2024JYCXJJ054.

Yuan Cao and Wei Peng are with the Huazhong University of Science and Technology, Wuhan 430000, China. Wei Peng is also with the research institue of Huazhong University of Science and Technology in Shenzhen, Shenzhen 518057, China. (e-mail:yuancao@hust.edu.cn; pengwei@hust.edu.cn).

Chau Yuen is with the School of Electrical and Electronics Engineering Nanyang Technological University, Singapore 639798. (e-mail: chau.yuen@ntu.edu.sg).

The corresponding author is Wei Peng

power is theoretical analyzed.

- The closed-form solutions for the optimal rotation angle and the critical rotation angle are derived.
- The RIS-reflected beamwidth decreases before the optimal rotation angle and increases thereafter, thus an enlarged receiving area is obtained and the UE movement within a certain range is allowed.
- The impact of phase errors in RIS units on the received power is considered. It is shown that the performance degradation can be effectively compensated by the proposed rotation scheme.

II. System Model

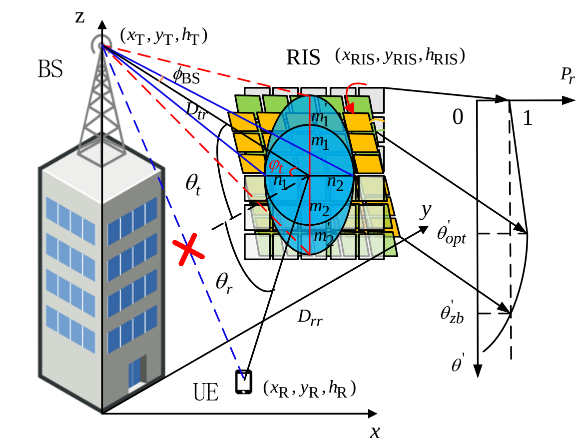

(a) (b)

Fig. 1: The Rotated RIS-aided Mmwave Communication System (a) System Model (b) Received Signal Power v.s. the Rotation Angle.

Considering a RIS-assisted millimeter-wave communication system, as shown in Fig. 1(a). The BS is located at the top of a building, the UE is located in the blind area of the BS, and the RIS is deployed to reflect the signal beam towards the UE. The BS is equipped with a large antenna array that can transmit a highly directional beam. The RIS is located in the far fields of both the BS and the UE, and the down tilt angle can be adjusted. Both the BS-to-RIS and RIS-to-UE links are line-of-sight (LoS) paths.

In the three-dimensional Cartesian coordinate system, the BS, the RIS center and the UE are denoted as $(x_{\mathrm{T}}, y_{\mathrm{T}}, h_{\mathrm{T}})$, $(x_{\mathrm{RIS}}, y_{\mathrm{RIS}}, h_{\mathrm{RIS}})$ and $(x_{\mathrm{R}}, y_{\mathrm{R}}, h_{\mathrm{R}})$ respectively. The RIS consists of M rows and N columns with angle-insensitive units, ensuring minimal impact on amplitude and phase performance at large incident angles [13]. Therefore, even with a non-orthogonal angle of incidence after rotation, the impact on performance is negligible. The length and width of the RIS unit are S_x and S_y, respectively. The azimuth angles of BS and UE relative to RIS are φ_t and φ_r, respectively. With the optimal beamforming, the phase $\phi_{m,n}$ of the m-th row and n-th column unit can be expressed as

$$\begin{aligned}\phi_{m,n} = \mathrm{mod}\bigg(-\frac{2\pi}{\lambda}\Big[&(\sin\theta_t\cos\varphi_t + \sin\theta_r\cos\varphi_r)(n-\frac{1}{2})S_x \\ &+ (\sin\theta_t\sin\varphi_t + \sin\theta_r\sin\varphi_r)(m-\frac{1}{2})S_y\Big],\ 2\pi\bigg)\end{aligned}, \tag{1}$$

where θ_t and θ_r are the incident and reflection angles of RIS, respectively. D_{tr} and D_{rr} represent the distance from the BS to the RIS center and the distance from the RIS center to the UE, respectively. According to the path loss model, which was experimentally validated under far-field conditions [14], the peak received power can be obtained as

$$P_r = P_t\frac{G_tG_r(MNS_xS_y)^2A^2}{16\pi^2D_{tr}^2D_{rr}^2}\cos\theta_t\cos\theta_r, \tag{2}$$

where P_r and P_t respectively represent the received power and transmitted power, G_t and G_r are respectively the gains of the BS and UE antennas. A is the amplitude of the unit. From the geometric relationship, $\theta_t = \arccos((y_{\mathrm{RIS}} - y_{\mathrm{T}})/D_{tr})$ and $\theta_r = \arccos((y_{\mathrm{RIS}} - y_R)/D_{rr})$, where $D_{tr} = \sqrt{(x_{\mathrm{T}} - x_{\mathrm{RIS}})^2 + (y_{\mathrm{T}} - y_{\mathrm{RIS}})^2 + (h_{\mathrm{T}} - h_{\mathrm{RIS}})^2}$, and $D_{rr} = \sqrt{(x_{\mathrm{RIS}} - x_{\mathrm{R}})^2 + (y_{\mathrm{RIS}} - y_{\mathrm{R}})^2 + (h_{\mathrm{RIS}} - h_{\mathrm{R}})^2}$.

As depicted in Fig. 1(a), the original RIS plane (gray plane) is without rotation, where the BS emits a highly directional beam, and only part of the RIS units are illuminated. The units along the vertical axis of the RIS are fully illuminated when the RIS is at the optimal position (green plane) with rotation angle θ'_{opt}, maximizing the number of effective units and resulting in the highest received signal power. The critical rotation plane (yellow plane) is at the rotation angle θ'_{zb}, where the received power is the same as that in the non-rotational position. For a clearer expression, we indicate the rotation direction of the RIS with a red arrow. Performance diagram can be found in Fig. 1(b). Half of the 3dB beamwidth of BS is denoted by ϕ_{BS}, where $2\phi_{\mathrm{BS}} \approx 1.22\lambda/R_{\mathrm{BS}}$, and R_{BS} is the aperture of the transmit antenna.

Due to the existence of 3D deviation, the shape of the main beam projected onto the RIS region is irregular, which is actually an asymmetric ellipse. To facilitate mathematical modeling, the projection surface is approximated as an quasi-ellipse. The semi-horizontal and semi-vertical axis are taken as the average values of the actual projection axis, defined as n_e and m_e, which can be calculated as $n_e = (n_1 + n_2)/2$ and $m_e = (m_1 + m_2)/2$, where $m_1 = \frac{D_{tr}\sin(\phi_{\mathrm{BS}})}{\cos(\theta_t - \phi_{\mathrm{BS}})}$, $m_2 = \frac{D_{tr}\sin(\phi_{\mathrm{BS}})}{\cos(\theta_t + \phi_{\mathrm{BS}})}$, $n_1 = \frac{D_{tr}\sin(\phi_{\mathrm{BS}})}{\sin(\varphi_t + \phi_{\mathrm{BS}})}$ and $n_2 = \frac{D_{tr}\sin(\phi_{\mathrm{BS}})}{\sin(\varphi_t - \phi_{\mathrm{BS}})}$ are the lengths of the axis projected onto the RIS asymmetric ellipse, respectively. The proof can be completed following steps similar to that presented in the Appendix A of [15]. Furthermore, the elliptical area can be calculated as $S_i = \pi n_e m_e$, and the peak received signal power can be rewritten as

$$P_r = P_t\frac{G_tG_r(S_i)^2A^2}{16\pi^2D_{tr}^2D_{rr}^2}\cos\theta_t\cos\theta_r. \tag{3}$$

III. Received Power and Beamwidth Control

According to (3), when the RIS is illuminated by a highly directional beam, only a limited number of units are illuminated to sense and reflect the signal. Additionally, the peak received power is proportional to the square of the illuminated area. In this paper, the down tilt rotation angle θ' of RIS is rotated to increase the number of the effective RIS units. To avoid signal obstruction caused by excessive RIS rotation, the range of θ' is set to be $\theta' \in (0, \pi/2 - \theta_t)$.

A. Power Control

***Theorem* 1.** *The illuminated area of the RIS is quasi-elliptical and increases gradually during the rotation process until the RIS units are fully illuminated in the vertical direction. The angle at which the received signal power reaches its maximum is the optimal rotation angle θ'_{opt}, which is determined by D_{tr}, ϕ_{BS}, M, S_y, θ_t and θ_r. Further rotation will result in performance degradation, until it becomes equal to that of the non-rotational scheme, the corresponding angle is the critical rotation angle θ'_{zb}.*

The following four lemmas are given to prove ***Theorem 1***.

***Lemma* 1.** *The main beam of the BS antenna is directed towards the center of the RIS. The horizontal axis of the illuminated elliptical area on the RIS remains unchanged, while the vertical axis continues to increase until the RIS is fully illuminated in the vertical direction.*

Proof: The illuminated area of RIS during its rotation process is given as $S'_i = \pi n_e m'_e$, where $m'_e = (m'_1 + m'_2)/2$, $m'_1 = \frac{D_{tr}\sin(\phi_{\mathrm{BS}})}{\cos(\theta_t+\theta'-\phi_{\mathrm{BS}})}$, $m'_2 = \frac{D_{tr}\sin(\phi_{\mathrm{BS}})}{\cos(\theta_t+\theta'+\phi_{\mathrm{BS}})}$. m'_e increases monotonically with θ', given as

$$m'_e = \frac{1}{2}D_{tr}\sin\phi_{\mathrm{BS}} \times \left[\frac{1}{\cos(\theta_t+\theta'+\phi_{\mathrm{BS}})} + \frac{1}{\cos(\theta_t+\theta'-\phi_{\mathrm{BS}})}\right]. \tag{4}$$

Defining $g(\theta')$ as

$$g(\theta') = \left[\frac{1}{\cos(\theta_t+\theta'+\phi_{\mathrm{BS}})} + \frac{1}{\cos(\theta_t+\theta'-\phi_{\mathrm{BS}})}\right], \tag{5}$$

then the derivation of (6) can be obtained

$$\frac{d[g(\theta')]}{d\theta'} = \left[\frac{\sin(\theta_t+\theta'+\phi_{\mathrm{BS}})}{\cos^2(\theta_t+\theta'+\phi_{\mathrm{BS}})} + \frac{\sin(\theta_t+\theta'-\phi_{\mathrm{BS}})}{\cos^2(\theta_t+\theta'-\phi_{\mathrm{BS}})}\right]. \tag{6}$$

It is assumed that the BS uses a phased array antenna to generate an ultra-narrow beam with a beam width less than 1°. It can be considered that $\theta_t >> \phi_{\mathrm{BS}}$, then it is not difficult to find that $d\left[g(\theta')\right]/d\theta' > 0$ is established when we omit the ϕ_{BS}, which completes the proof of ***Lemma 1***. ■

Therefore, as θ' increases, the vertical illuminated area will gradually be expanded. The optimization problem is formulated as

$$\begin{aligned} \text{(P1)}\quad & \max_{\theta'}\ P'_r = P_t\frac{G_tG_r(S'_i)^2A^2}{16\pi^2D_{tr}^2D_{rr}^2}\cos(\theta_t+\theta')\cos(\theta_r-\theta') \\ \text{s.t.}\quad & 0<\theta_t,\theta_r<\pi/2 \\ & 0<\theta'<\pi/2-\theta_t \end{aligned}. \tag{7}$$

The received signal power will reach the maximum at the optimal rotation angle, and begins to decline by further rotation. It will be equal to the original value (without rotation) at the critical angle. The optimal angle and critical angle will be derived by ***Lemma 2*** and ***Lemma 3*** respectively.

***Lemma* 2.** *The optimal rotation angle is given by*

$$\theta'_{opt} = \begin{cases} \arccos\frac{2D_{tr}\sin\phi_{\mathrm{BS}}}{MS_y} - \theta_t, \theta'_e < \theta'_f \\ (\theta_r-\theta_t)/2 \qquad ,\theta'_e > \theta'_f \end{cases} \tag{8}$$

Proof: Since the ϕ_{BS} is very small and can be ignored in the denominator of m'_1 and m'_2, therefore, the optimization objective function of (7) can be reformulated as

$$P'_r = \underbrace{P_t\frac{G_tG_rn_e^2\sin^2\phi_{\mathrm{BS}}A^2}{16D_{rr}^2}}_{\alpha}\underbrace{\frac{\cos(\theta_t+\theta')\cos(\theta_r-\theta')}{\cos^2(\theta_t+\theta')}}_{\beta}, \tag{9}$$

where α is a constant, and β is a variable related to the incident angle, reflect angle and rotation angle when the positions of BS, RIS and UE are fixed, and the β can be redefined as

$$\beta(\theta') = \cos(\theta_r-\theta')/\cos(\theta_t+\theta'), \tag{10}$$

the derivative of (10) is then given by

$$d[\beta(\theta')]/d\theta' = \sin(\theta_t+\theta_r)/\cos^2(\theta_t+\theta'). \tag{11}$$

Due to $\theta_t,\theta_r \in (0,\pi/2)$, it can be observed that $\beta(\theta')$ is greater than 0 over the entire domain of definition. Thus, the received power increases with θ'.

However, when the illumination area of RIS remains unchanged, all units of the RIS in the vertical direction are illuminated under this condition, then the vertical axis of illuminated elliptical region is $m'_e = MS_y/2$, the equivalent expression is

$$\frac{1}{2}\left[\frac{D_{tr}\sin\phi_{\mathrm{BS}}}{\cos(\theta_t+\theta'+\phi_{\mathrm{BS}})} + \frac{D_{tr}\sin\phi_{\mathrm{BS}}}{\cos(\theta_t+\theta'-\phi_{\mathrm{BS}})}\right] = MS_y/2. \tag{12}$$

Similarly, ϕ_{BS} is omitted in the denominator, the rotation angle obtained in this case can be calculated as

$$\theta'_f = \arccos\frac{2D_{tr}\sin\phi_{\mathrm{BS}}}{MS_y} - \theta_t. \tag{13}$$

Furthermore, the maximum received power is given by

$$P'_r = \underbrace{P_t\frac{G_tG_r(n_em'_e)^2A^2}{16D_{tr}^2D_{rr}^2}}_{\kappa}\cos(\theta_t+\theta')\cos(\theta_r-\theta'), \tag{14}$$

where κ is a constant, and the variable is defined as

$$\vartheta(\theta') = \cos(\theta_t+\theta')\cos(\theta_r-\theta'), \theta' \in [\theta'_f, \pi/2-\theta_t]. \tag{15}$$

Then the derivative of (15) is $d[\vartheta(\theta')]/d\theta' = 0$, when $\theta' = (\theta_r-\theta_t)/2$, we have $\vartheta'(\theta') = 0$. The extreme point is defined as $\theta'_e = (\theta_r-\theta_t)/2$. To achieve a larger range of rotation angles, let us assume $\theta_r > \theta_t$, there are two possible cases:

Case 1. *If $\theta'_e < \theta'_f$, the received power starts to attenuate within $\theta' \in [\theta'_f, \pi/2-\theta_t]$, the optimal rotation angle is θ'_f.*

Case 2. *If $\theta'_e > \theta'_f$, then $\theta' \in [\theta'_f, \theta'_e]$, $\vartheta(\theta') > 0$, the received power is maximized at θ'_e. The received power starts to attenuate within $\theta' \in [\theta'_e, \pi/2-\theta_t]$, and the optimal rotation angle is θ'_e.*

The optimal rotation angle can be obtained and then the received signal power can be calculated by (9), the objective function in (P1) is unimodal, this ends the proof. ■

Actually, $\theta^{'}_{zb}$ represents the zero boundary point for the improvement of the signal strength. When the rotation angle is less than $\theta^{'}_{zb}$, the signal strength can be improved within this range, while further rotation will degrade the performance.

***Lemma* 3.** *The critical rotation angle is given by*

$$\theta^{'}_{zb} = \frac{1}{2} \times \left[\arccos\left(\frac{8D_{tr}^2 \sin^2\phi_{\mathrm{BS}} \cos\theta_r}{M^2 S_y^2 \cos\theta_t} - \cos(\theta_t + \theta_r)\right) - \theta_t + \theta_r\right]. \tag{16}$$

Proof: From the previous analysis, it can be seen that if the RIS continues to rotate after the optimal angle, the received power begins to decrease. At this stage, the received power of the UE may equal that of the non-rotation scheme. It can be formulated and simplified as

$$(m_e)^2 \cos\theta_t \cos\theta_r = (m_e^{'})^2 \cos(\theta_t + \theta^{'}) \cos(\theta_r - \theta^{'}). \tag{17}$$

Furthermore, $m_e^{'} = MS_y/2$, and the ϕ_{BS} is omitted in the denominator of m_e, so (17) can be reformulated as

$$\frac{D_{tr}^2 \sin^2\phi_{\mathrm{BS}} \cos\theta_r}{\cos\theta_t} = \left(\frac{MS_y}{2}\right)^2 \cos(\theta_t + \theta^{'}) \cos(\theta_r - \theta^{'}). \tag{18}$$

According to the sum-to-product identities of cosine, we have

$$\frac{D_{tr}^2 \sin^2\phi_{\mathrm{BS}} \cos\theta_r}{\cos\theta_t} = \frac{1}{2}\left(\frac{MS_y}{2}\right)^2 \times \left[\cos(\theta_t + \theta_r) + \cos(\theta_t - \theta_r + 2\theta^{'})\right]. \tag{19}$$

The inverse trigonometric function is used to obtain the (16), this completes the proof. ■

Discussions: It should be noted that the above three lemmas are derived under the assumption of a particularly small ϕ_{BS}, which was then omitted during the derivation to obtain the closed-form expressions. In practice, when ϕ_{BS} exceeds $5°$, this approximation may introduce noticeable modeling errors that can affect the accuracy of the results. Therefore, the proposed model is applicable when $\phi_{\mathrm{BS}} \leq 5°$, which is typical in high-gain millimeter wave systems. Scenarios with wider beams should be addressed using more general models.

B. 3dB Beamwidth Control

The change in the illuminated area affects the vertical number of effective units during the rotation, which in turn affects the 3dB beamwidth of the reflected beam. The number of vertical units can be approximated as $M^{'} = \left\lfloor S_i^{'}/2n_e S_y \right\rfloor$, and the horizontal units $N^{'}$ can be calculated as the same way. The 3dB beamwidth is twice the deviation of the reflection and incident angles.

***Lemma* 4.** *The angle deviation of the reflected beam is denoted as*

$$\left|\theta_r^{'} - \theta_t^{'}\right| = \sqrt{\frac{3}{2}} \frac{\lambda}{\pi M^{'} S_y \cos\theta_t^{'}}, \tag{20}$$

where $\theta_t^{'} = \theta_t + \theta^{'}$ and $\theta_r^{'} = \theta_r - \theta^{'}$ respectively represent the incident and reflection angles of RIS after rotation. The number of RIS units along the vertical axis increases with the rotation, while $\cos\theta_t^{'}$ continuously decreases, which will widen the beamwidth.

Proof: According to [14], assuming all RIS units are with the same amplitude A and the different phase shift, the received signal power can be given as

$$P_r^{'} = \frac{P_t G_t G_r (M^{'} N^{'} S_x S_y)^2 \cos\theta_t^{'} \cos\theta_r^{'} A^2}{16\pi^2 D_{tr}^2 D_{rr}^2} |\Xi|^2, \tag{21}$$

where Ξ is defined as (22) at the top of the next page. Specially, when the azimuth angles of the transmit antenna and the receive antenna are respectively $\pi/2$ and $3\pi/2$, as well as $\mathrm{sinc}(\,\cdot\,)$ is an even function, so Ξ can be simplified. The Taylor expansions of the cosine function and the triangle identical transformation are used as follows

$$\sin\theta_r^{'} - \sin\theta_t^{'} = (\theta_r^{'} - \theta_t^{'}) \cos\theta_t^{'} + O((\theta_r^{'} - \theta_t^{'})^2). \tag{23}$$

In addition, $\mathrm{sinc}^2(x) = 1 - x^2/3 + O(x^3)$. Furthermore, the half-power beamwidth is the angle range corresponding to when the received power decreases from its peak to half of its maximum, then $|\Xi|^2 = 1/2$ can be obtained and rewritten as

$$|\Xi|^2 = \frac{1 - \frac{(M^{'})^2 \pi^2 S_y^2}{\lambda^2} \frac{(\theta_r^{'} - \theta_t^{'})^2 \cos^2\theta_t^{'}}{3}}{1 - \frac{\pi^2 S_y^2}{\lambda^2} \frac{(\theta_r^{'} - \theta_t^{'})^2 \cos^2\theta_t^{'}}{3}} = \frac{1}{2} \tag{24}$$

Accordingly, it can be simplified as

$$\frac{\pi^2 S_y^2 \cos^2\theta_t^{'} (\theta_r^{'} - \theta_t^{'})^2}{3\lambda^2} \left[(M^{'})^2 - \frac{1}{2}\right] = \frac{1}{2} \tag{25}$$

Since $(M^{'})^2 >> 1/2$, $\left[(M^{'})^2 - 1/2\right] \approx (M^{'})^2$, substitute it into (25) to obtain the (20). ■

IV. Failure Analysis

In this section, we consider the impact of random failure of RIS units on the received signal power, and the random phase shift error function can be expressed as

$$F_{m,n} = \begin{cases} 1, & \text{if the unit is functioning} \\ e^{j\delta}, & \text{if the unit is faulty} \end{cases}, \tag{26}$$

where $\delta \sim \mathcal{U}[0, 2\pi]$, and $\mathcal{U}[a, b]$ denotes a uniform distribution over the interval $[a, b]$ [16]. The reflection coefficient of the illuminated unit is $Ae^{j\phi_{m,n}}$. Then the received power in the presence of random phase shift errors can be expressed as

$$P_f = P_t \frac{G_t G_r (S_x S_y)^2 A^2 \cos\theta_t \cos\theta_r}{16\pi^2 D_{tr}^2 D_{rr}^2} |\Lambda|^2, \tag{27}$$

where Λ is defined in (28) at the top of the next page, and $\phi_{m,n}$ denotes the optimal phase shift obtained from (1). And the received power after rotation can be denoted as $P_f^{'}$, which can be calculated by substituting $\theta_t^{'}$ and $\theta_r^{'}$ into (27). In addition, the critical rotation angle of failure compensation is defined as $\theta_c^{'}$, it can be obtained by making $\left|P_f^{'} - P_r\right| < \epsilon$.

V. Simulation Results

In this section, we testify the performance of the proposed method and verify the ***Theorem 1*** by numerical calculations.

$$\Xi = \frac{\mathrm{sinc}\left(\frac{N' \pi S_x}{\lambda}(\sin\theta_t' \cos\varphi_t + \sin\theta_r' \cos\varphi_r)\right)}{\mathrm{sinc}\left(\frac{\pi S_x}{\lambda}(\sin\theta_t' \cos\varphi_t + \sin\theta_r' \cos\varphi_r)\right)} \frac{\mathrm{sinc}\left(\frac{M' \pi S_y}{\lambda}(\sin\theta_t' \sin\varphi_t + \sin\theta_r' \sin\varphi_r)\right)}{\mathrm{sinc}\left(\frac{\pi S_y}{\lambda}(\sin\theta_t' \sin\varphi_t + \sin\theta_r' \sin\varphi_r)\right)} \tag{22}$$

$$\Lambda = \sum_{m=1-\frac{M'}{2}}^{\frac{M'}{2}} \sum_{n=1-\frac{N'}{2}}^{\frac{N'}{2}} e^{j\left[\frac{2\pi\left((\sin\theta_t \cos\varphi_t + \sin\theta_r \cos\varphi_r)\left(n-\frac{1}{2}\right)S_x + (\sin\theta_t \sin\varphi_t + \sin\theta_r \sin\varphi_r)\left(m-\frac{1}{2}\right)S_y\right)}{\lambda}\right]} e^{j\phi_{m,n}} \cdot F_{m,n} \tag{28}$$

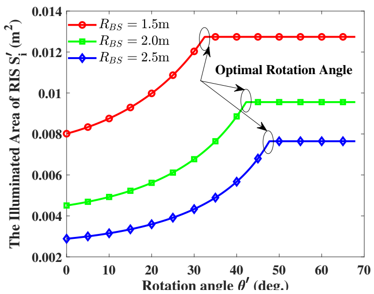

Fig. 2: The illuminated area of RIS v.s. different θ'.

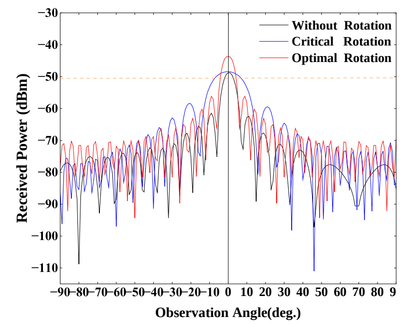

Fig. 4: The received power with $R_{\mathrm{BS}} = 1.5$m.

The simulation parameters are x_{T}=0m, y_{T}=0m, h_{T}=12m, x_{RIS}=0m, x_{R}=10m, y_{R}=0m, h_{R}=0m, $M = N = 30$, $G_t = G_r = 20.4$dB, $P_t = 0.1$W, $A = 0.9$ is set due to the practical physical limitation of RIS units, $S_x = S_y = \lambda/2$ and the system operating frequency is $f = 27$GHz. RIS will obtain the a greater degree of freedom of the down tilt angle if its height is similar to the BS. For example, when the $h_{\mathrm{RIS}} = 8$m and $y_{\mathrm{RIS}} = 10$m, the incident and reflect angle can be calculated as $\theta_t = 21.8^\circ$ and $\theta_r = 52^\circ$, respectively.

Fig. 2 considers the influence of the rotation angle θ' on the effective illuminated area of RIS S_i' under different aperture of BS antenna R_{BS}. The S_i' will remain constant while the RIS is at its optimal rotation angle. According to (8), when the apertures of the base station antenna are $R_{\mathrm{BS}} = 1.5$ m, 2.0 m and 2.5 m, the optimal rotation angles of the RIS can be calculated as 32.47°, 42.22°, and 47.69°, respectively. Theoretical calculations are consistent with the simulations. In addition, the transmit signal beamwidth narrows as the R_{BS} increases, and a larger rotation angle is required to achieve a constant S_i'.

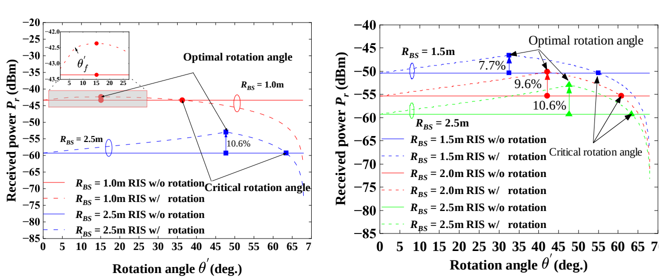

(a) (b)

Fig. 3: P_r v.s. θ' (a) under two cases (b) under different R_{BS}.

As depicted in Fig. 3(a), two cases of ***Lemma 2*** are first analyzed, the blue curve represents ***Case 1***, where the peak received signal power is maximized when the RIS is at its optimal angle, after which it begins to attenuate. The red curve represents ***Case 2***, where the peak received signal power is not maximized when the vertical RIS units are completely illuminated (as indicated by θ_f'). Instead, the power reaches its peak when the RIS is further rotated to $(\theta_r - \theta_t)/2$=15.1°, indicating that in this case, further rotation of RIS can provide extra performance gain. Fig. 3(b) analyzes the influence of different RIS rotation angles on the received power under three different R_{BS}. When D_{tr} is same, the larger the R_{BS}, the smaller the received signal power. When the BS antenna apertures are $R_{\mathrm{BS}} = 1.5$ m, 2 m and 2.5 m, the critical rotation angles are respectively 55.11°, 60.81° and 63.44°, which are identical to the calculation results (16), and the received signal power can be improved by 7.7%, 9.6% and 10.6%, respectively. The performance will be degraded after the critical rotation and will even be worse than the non-rotational scheme.

To validate the variation in the beamwidth of the reflected beam during rotation, Fig. 4 simulates the received power curves during the rotation process under the condition of $R_{\mathrm{BS}} = 1.5$m, $x_{\mathrm{R}} = 0$m and $y_{\mathrm{R}} = 3$m. To simplify the comparison, the main beam peaks are aligned at 0°, it can be observed that the peak received signal power at its optimal rotation angle are improved. While at the critical rotation angle, it achieves approximately four times beamwidth compared to the non-rotational scheme, and the received power performance is maintained at the same time.

To demonstrate the effectiveness of the proposed scheme, the received power under the optimal beamforming is compared with two baseline schemes: 1) Optimal RIS location without rotation [3]; 2) Optimal RIS location with optimal rotation angle [7]. Two scenarios are considered in our sim-

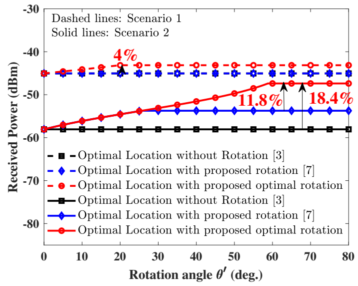

Fig. 5: Comparison of received power with $R_{\mathrm{BS}} = 1.5\,\mathrm{m}$.

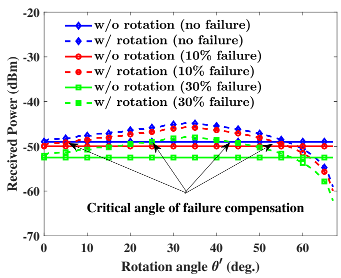

Fig. 6: Failure compensation for the received power with $R_{\mathrm{BS}} = 1.5$m.

ulation. **Scenario1:** $y_{\mathrm{RIS}} = 10$m, the optimal location for deploying the RIS should be at the midpoint between the BS and the UE. **Scenario2:** $y_{\mathrm{RIS}} = 4$m, the optimal location of the RIS shifts to the BS side. The received power curves are simulated under the condition of $x_{\mathrm{R}} = 0$m, $y_{\mathrm{R}} = 0$m, other parameters are the same as previously mentioned. The optimal locations of RIS can be calculated as (0,10,6) and (0,4,10.47), respectively. The RIS stops rotating at the optimal angle. The proposed method demonstrates significant potential in enhancing the performance. As shown in Fig. 5, the two baseline schemes exhibit identical performance in Scenario 1, where the proposed scheme achieves an improvement of approximately 4%. In Scenario 2, performance gains of 11.8% and 18.4% over the two baseline schemes are achieved.

Finally, random errors in RIS units are introduced, and the effectiveness of the proposed scheme to compensate for the received power is illustrated in Fig. 6. In the simulations, $\epsilon = 0.1$, and random phase errors are introduced to part of the units (with percentage 10% and 30%) at each rotation angle based on (27). It can be observed that, the phase errors will decrease the received power. For example, 30% failure results in a 3.6 dB loss in the received power. However, the proposed rotation strategy can effectively compensate for the degradation, restoring performance at rotation angles of 24° and 43°, and providing consistent gains within this range.

VI. Conclusions

In this paper, a rotation optimization method to improve the peak received power of the millimeter wave high directional communication system is proposed. The RIS is partially illuminated by the transmit beam, resulting in poor received power at the UE. To address this issue, the optimal and critical rotation angles are first derived. Additionally, the received power as a function of the rotation angle is theoretically analyzed. Then, the 3 dB beamwidth of the reflected beam is derived. Finally, random phase errors are introduced to the RIS units to evaluate the effectiveness of the proposed rotation strategy in compensating for the loss in the received power. The simulation results validate the effectiveness of the proposed method. The received signal power can be improved and the 3dB beamwidth of the reflected beam can be controlled. An interesting direction for future work is to extend the analysis to more complicated mmWave channel condition, especially those with rich-scattering or non-LoS scenarios.

References

[1] Y. Cheng, C. Huang, W. Peng, M. Debbah, L. Hanzo, and C. Yuen, "Achievable Rate Optimization of the RIS-Aided Near-Field Wideband Uplink," *IEEE Trans. Wireless Commun.*, vol. 23, pp. 2296–2311, Mar 2023.

[2] Q. Wu, S. Zhang, B. Zheng, C. You, and R. Zhang, "Intelligent Reflecting Surface-Aided Wireless Communications: A Tutorial," *IEEE Trans. Commun.*, vol. 69, no. 5, pp. 3313–3351, May. 2021.

[3] Y. Ren, R. Zhou, X. Teng, S. Meng, M. Zhou, W. Tang, X. Li, C. Li, and S. Jin, "On Deployment Position of RIS in Wireless Communication Systems: Analysis and Experimental Results," *IEEE Wireless Commun. Lett.*, vol. 12, no. 10, pp. 1756–1760, Oct. 2023.

[4] K. Ntontin, A.-A. A. Boulogeorgos, D. G. Selimis, F. I. Lazarakis, A. Alexiou, and S. Chatzinotas, "Reconfigurable Intelligent Surface Optimal Placement in Millimeter-Wave Networks," *IEEE Open J. Commun. Soc.*, vol. 2, pp. 704–718, Apr. 2021.

[5] Z. Cui, K. Guan, J. Zhang, and Z. Zhong, "SNR Coverage Probability Analysis of RIS-Aided Communication Systems," *IEEE Trans. Veh. Technol.*, vol. 70, no. 4, pp. 3914–3919, Apr. 2021.

[6] S. Zeng, H. Zhang, B. Di, Z. Han, and L. Song, "Reconfigurable Intelligent Surface (RIS) Assisted Wireless Coverage Extension: RIS Orientation and Location Optimization," *IEEE Commun. Lett.*, vol. 25, no. 1, pp. 269–273, Jan. 2021.

[7] Y. Cheng, W. Peng, G. C. Alexandropoulos, and M. Debbah, "RIS-Aided Wireless Communications: Extra Degrees of Freedom via Rotation and Location Optimization," *IEEE Trans. Wireless Commun.*, vol. 21, no. 8, Feb. 2022.

[8] S. Xu, H. Guo, W. Dong, and B. Lyu, "Optimal Elevation and Azimuth Rotation for RIS-Assisted Wireless Transmission," *IEEE Commun. Lett.*, vol. 28, no. 12, pp. 2909–2913, Oct. 2024.

[9] W. Chen, X. Yang, C.-K. Wen, W. Tang, J. Wang, Y. Yuan, X. Li, and S. Jin, "Rotatable Block-Controlled RIS: Bridging the Performance Gap to Element-Controlled Systems," *IEEE Commun. Lett.*, vol. 29, no. 1, pp. 185–189, Nov. 2024.

[10] K. Wang, C.-T. Lam, and B. K. Ng, "Reconfigurable Intelligent Surface Assisted Communications Using Dynamic Rotations," in *Proc. IEEE Int. Conf. Commun. Technol. (ICCT)*, Nanjing, China, Nov. 2022, pp. 652–656.

[11] Y. Cao, J. Li, and W. Peng, "Off-Center Optimization for Reconfigurable Intelligent Surface: Design and Experiments," in *Proc. IEEE Int. Conf. Commun. (ICC)*, Denver, CO, USA, Jun. 2024, pp. 4366–4371.

[12] K. Ntontin, D. Selimis, A.-A. A. Boulogeorgos, A. Alexandridis, A. Tsolis, V. Vlachodimitropoulos, and F. Lazarakis, "Optimal Reconfigurable Intelligent Surface Placement in Millimeter-Wave Communications," in *Proc. Eur. Conf. Antennas Propag. (EuCAP)*, Düsseldorf, Germany, Mar. 2021, pp. 1–5.

[13] L. Zhang and T. J. Cui, "Angle-insensitive 2-bit programmable coding metasurface with wide incident angles," in *Proc. IEEE Asia–Pacific Microw. Conf. (APMC)*, Singapore, Dec. 2019, pp. 932–934.

[14] W. Tang, X. Chen, M. Z. Chen, J. Y. Dai, Y. Han, M. D. Renzo, S. Jin, Q. Cheng, and T. J. Cui, "Path Loss Modeling and Measurements for Reconfigurable Intelligent Surfaces in the Millimeter-Wave Frequency Band," *IEEE Trans. Commun.*, vol. 70, no. 9, pp. 6259–6276, Sep. 2022.

[15] Z. Cui and S. Pollin, "Impact of Reconfigurable Intelligent Surface Geometry on Communication Performance," *IEEE Wireless Commun. Lett.*, vol. 12, no. 5, pp. 898–902, May. 2023.

[16] C. Ozturk, M. F. Keskin, V. Sciancalepore, H. Wymeersch, and S. Gezici, "RIS-Aided Localization Under Pixel Failures," *IEEE Trans. Wireless Commun.*, vol. 23, no. 8, pp. 8314–8329, Jan. 2024.